

Effect of hydrolysis conditions on hydrous TiO₂ polymorphs precipitated from a titanyl sulfate and sulfuric acid solution

Hao Song, Bin Liang, Li Lü, Pan Wu, and Chun Li

Department of Metallurgical Engineering, Sichuan University, Chengdu 610065, China

(Received: 15 August 2011; revised: 28 October 2011; accepted: 7 November 2011)

Abstract: The relationship between hydrolysis conditions and hydrous titania polymorphs obtained in a titanyl sulfate and sulfuric acid solution was investigated by X-ray diffraction (XRD), scanning electron microscopy (SEM), and high-resolution transmission electron microscopy (HRTEM). The results revealed that the feeding rate of the titanyl sulfate stock solution, the concentration of sulfuric acid, and the seed dosage of rutile crystal could significantly affect the hydrolysis rate, thus influencing the titania crystal phase. Hydrous TiO₂ in the form of rutile, anatase, or the mixture of both could be obtained in solutions of low titanium concentrations and 2.5wt% to 15wt% sulfuric acid at 100°C. When the hydrolysis rate of titanium expressed by TiO₂ was more than or equal to 0.04 g/(L·min), the hydrolysate was almost phase-pure anatase, while the main phase state was rutile when the hydrolysis rate was less than or equal to 0.01 g/(L·min). With the hydrolysis rate between 0.02 and 0.03 g/(L·min), the hydrolysate contained almost equal magnitude of rutile and anatase. It seems that although rutile phase is thermodynamically stable in very acidic solutions, anatase is a kinetically stable phase.

Keywords: titanium dioxide; titanyl sulfate; sulfuric acid; hydrolysis; anatase; rutile

[This work was financially supported by a grant from the Ph.D. Programs Foundation of the Ministry of Education of China (No. 20070610125).]

1. Introduction

Titania is widely used due to its peculiar physicochemical properties applicable to various scientific and technical fields and exists in three crystal phases: rutile, anatase, and brookite. Titania with a rutile structure is the most widely used because of its high refractive index, tinting strength, and inert chemical properties. The anatase form is preferred as a photocatalyst used for the purification of water and air [1-3] and titania membrane applications in dye-sensitized titanium oxide solar cells [4]. Thus, controlling the crystal phase of titania is of great importance from the viewpoint of potential applications [5].

TiO₂ is commercially produced by two methods, *i.e.*, sulfate process and chloride process. Generally, hydrous titania with anatase is obtained in the hydrolysis section of the

sulfate process, while in the high-temperature chloride process the rutile form is obtained.

To understand the thermodynamic phase stability of TiO₂, a great deal of work was involved [6-14]. It has been found that the phase stability of nanosized TiO₂ is size dependent in air [7]. The stability in aqueous solutions was also explored. Yanagisawa and Ovenstone [15] demonstrated that the protonation degree of TiO₂ surfaces increased with the increase of acid concentration, leading to dissolution of anatase and formation of rutile. Finnegan *et al.* [16] showed that the stability of TiO₂ phase strongly depended on pH values. At small size, rutile is more stable than anatase phase in very acidic solutions. Clearly, rutile is thermodynamically more stable in acid solutions.

Also, quite a lot of work focused on the relationship between polymorph phases of hydrous TiO₂ and hydrolysis

Corresponding author: Chun Li E-mail: lic@scu.edu.cn

© University of Science and Technology Beijing and Springer-Verlag Berlin Heidelberg 2012

conditions in aqueous solutions. Majority of them were dedicated to aqueous chloride systems using TiCl₄ [17-19], TiCl₃ [20], or TiOCl₂ [21] as precursors. Few examined the relationship in sulfuric acid systems, although the hydrolysis of titanyl sulfate solutions was widely investigated [22-24].

In the present work, hydrolyzing a titanyl sulfate stock solution in 2.5wt% to 15wt% sulfuric acid solutions was studied. The effects of hydrolysis conditions such as the feeding speed of the titanyl sulfate stock solution, the concentration of sulfuric acid, and the dosage of crystal seeds on the crystal phase of hydrous TiO₂ were investigated.

2. Experimental

2.1. Hydrolysis experiment

Hydrolysis of the titanyl sulfate solutions was carried out in a four-necked flask equipped with an agitator, a condenser, and a thermometer. The fourth opening was used to feed reactants and withdraw reacting slurry samples. The flask was heated using an oil bath with a temperature fluctuation within $\pm 2^\circ\text{C}$. In each experiment, a 300 mL sulfuric acid solution with different concentrations was first introduced to the flask and preheated to 100°C . A total of 9 or 18 mL titanyl sulfate stock solution with a TiO₂ concentration of 200 g/L was added at a certain constant speed using a peristaltic pump (BT50-1J, Baoding Longer Precision Pump Co., Ltd., China) with an allowable error of less than 5%. The total reaction time including both the stock solution feeding (the titanium hydrolysis occurred during the feeding) and subsequent annealing time was fixed at 9 h unless otherwise specified. The agitation was kept constant at 150 ± 10 r/min during the entire hydrolysis operation.

A 2 mL hydrolytic slurry sample was periodically withdrawn, rapidly cooled, filtered, and washed with a 5wt% H₂SO₄ solution. Having been fixed up volumetrically, the as-prepared solution was chemically analyzed. At the end of each test, all the remainder reacting slurry was filtered and washed first by a dilute solution then deionized water. The solid sample thus obtained was collected and dried at 100°C for characterization.

Rutile crystal seeds were obtained by dripping 50 mL of 1 mol/L sodium hydroxide solution into 20 mL of 0.625 mol/L TiCl₄ solution at room temperature. The white precipitate obtained was washed until all the impurities were removed and then dispersed in deionized water and kept for later usage.

2.2. Analysis and characterization

The titanium ion concentration in reacting solutions was determined using reduction-oxidation titration [25]. The hydrolysates were subjected to X-ray diffraction (XRD) analysis (DX-1000 diffractometer, Dan. Instrument Co., Ltd., China). The voltage and anode current used were 45 kV and 25 mA, respectively. The K_α of the copper target is 0.15405 nm and the continuously scanning mode with 0.06 intervals was used to collect the XRD patterns of the samples over a 2θ range of 20° to 80° . The mass fractions of rutile and anatase phase in these solid samples were calculated with the XRD data by using the Rietveld whole pattern fitting method [26-30], which was embedded in MAUD software.

The grain size was determined using the Scherrer equation, $L = K\lambda/\beta\cos\theta$, where L is the average grain size (nm), λ is the wavelength of X-ray radiation (0.154056 nm for the copper target), K is a constant usually taken as 0.9, and θ is the diffracting angle. $\beta = B - b$, where b is the peak width (full width at half-maximum, FWHM) of a standard sample (the crystallites must be larger than 1 nm) and B is the FWHM for samples at the peak position given by the scattering angle 2θ .

The morphology of the hydrolysates was observed using an S-450 scanning electron microscope (SEM, Hitachi, Japan) at an accelerating voltage of 20 kV. High-resolution transmission electron microscopy (HRTEM) images of the samples were taken with a JEM-3010 transmission electron microscope (JEOL, Japan) at an accelerating voltage of 200 kV.

3. Results

3.1. Effect of the feeding rate of the titanyl sulfate stock solution

A series of tests was conducted in 5% H₂SO₄ solution at 100°C . The applied feeding rates were 1, 2, 4, and 8 mL/h. Thus, in the former two occasions, it took up 9 h to add total 9 and 18 mL titanyl sulfate stock solution, respectively, without subsequent annealing, while in the latter two occasions it took up 4.5 and 2.25 h, respectively, to add 18 mL titanyl sulfate stock solution and then the reacting slurry continuously annealed up to 9 h.

Fig. 1 shows the variation of Ti⁴⁺ concentration in the reacting slurry with time at different feeding rates. In each test, the titanium concentration increased first and then decreased due to evident hydrolysis after reaching a certain supersaturation. The supersaturation increased with increasing feed-

ing rate. Based on Fig. 1, the hydrolysis fraction (ratio of hydrolyzed titanium to total titanium added in the reacting time of 9 h) was calculated and its variation with time is shown in Fig. 2. It can be seen that once the hydrolysis launched it progressed almost at a constant rate, as indicated by the straight-line changes in the primary hydrolysis stages. It speeded with increasing feeding rate.

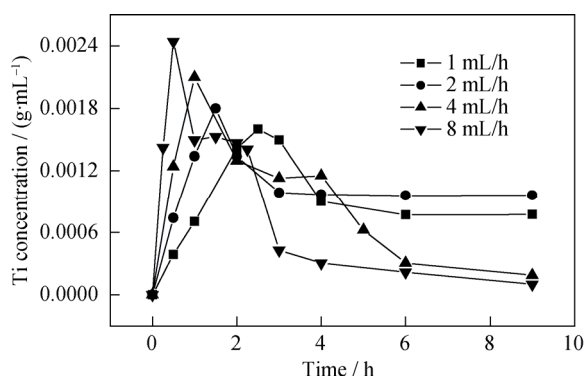


Fig. 1. Variation of the titanium concentration of the reacting slurry with time at different titanium feeding rates.

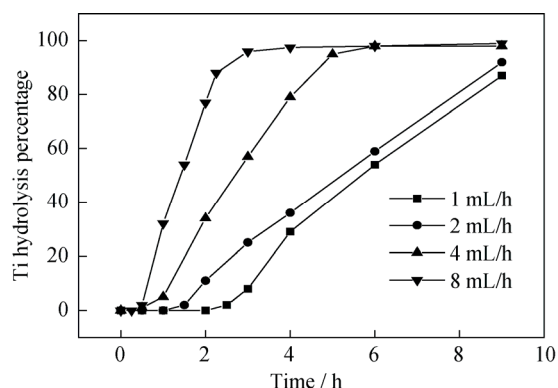


Fig. 2. Variation of the hydrolysis percentage with time at different titanium feeding rates.

Fig. 3 demonstrates the XRD patterns of hydrolysates obtained in 9 h of reaction at different feeding rates. All the peaks were well matched with the phases of rutile (pdf card No. 65-0190) and anatase (pdf card No. 21-1272), and no brookite (pdf card No. 29-1360) was detected. The peak intensity of rutile gradually increased with decreasing feeding rate, while that of anatase exhibited an opposite trend. The mass fraction and crystallite size of anatase and rutile phase in the hydrolysates were calculated quantitatively from the XRD patterns and are listed in Table 1. The feeding rate of the titanium stock solution significantly influenced the crystal phase of hydrolysates. For the hydrolysate obtained at a feeding rate of 8 mL/h, anatase was the predominant phase with only 2wt% of rutile. With the decrease of feed-

ing rate, the content of rutile phase rapidly increased. For the hydrolysate obtained at a feeding rate of 1 mL/h, the rutile content reached up to 92wt%. On the other hand, the feeding rate affected the crystallite size only to some extent with the size ranging from 6 to 11 nm for anatase and 4 to 6 nm for rutile.

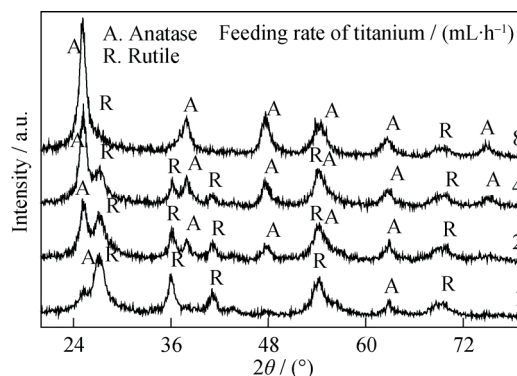


Fig. 3. XRD patterns of hydrolysates at different titanium feeding rates.

Table 1. Variation of the phase composition and crystallite size of hydrolysates with titanium feeding rate

Feeding rate / (mL·h ⁻¹)	Composition / wt%		Crystallite size / nm	
	Anatase	Rutile	Anatase	Rutile
1	8	92	6	6
2	35	65	9	6
4	48	52	11	4
8	98	2	10	—

Fig. 4 shows the SEM photos of hydrolysates obtained at different feeding rates. Hydrolysate samples obtained at feeding rates of 1 and 2 mL/h were spherical with average sizes of about 5 and 2 μm, respectively. With the feeding rate increasing up to 8 mL/h, the particle size decreased to only about 1 μm and the morphology became irregular and rough. Clearly, high feeding rate resulted in high hydrolysis rate (see Fig. 2), which generated a great deal of minute hydrolytic particles.

HRTEM images of hydrolysate samples obtained at feeding rates of 1 and 8 mL/h are shown in Fig. 5. The corresponding crystallite sizes are about 10 and 5 nm, respectively. The results are well consistent with the values calculated from XRD analysis (see Table 1), indicating that the crystallite size estimated based on XRD analysis is reliable. Therefore, the XRD estimation method was used hereafter.

3.2. Effect of reaction time

A series of tests was conducted in 5wt% sulfuric acid

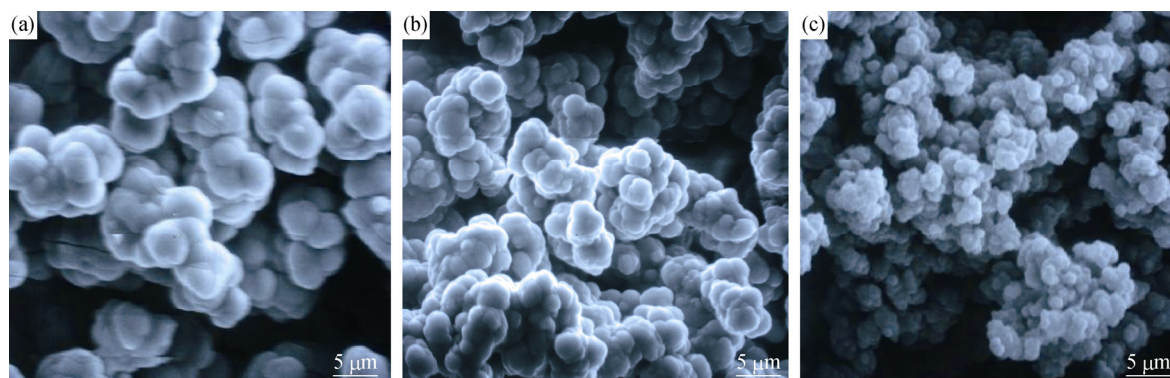


Fig. 4. SEM images of hydrolysates at different titanium feeding rates: (a) 1 mL/h; (b) 2 mL/h; (c) 8 mL/h.

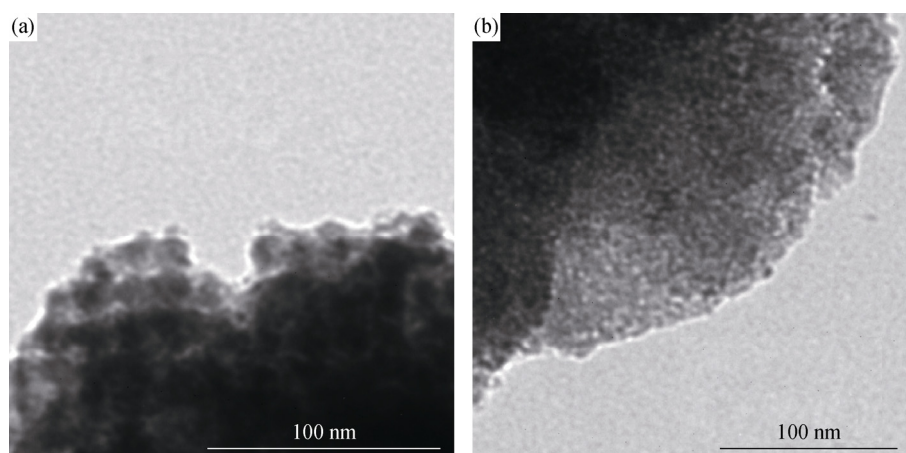


Fig. 5. HRTEM images of hydrolysates at different titanium feeding rates: (a) 1 mL/h; (b) 8 mL/h.

solution at 100°C with the feeding rate of 2 mL/h of the titanyl sulfate stock solution. XRD patterns of hydrolysates obtained at different reaction time durations are shown in Fig. 6. The peak intensity for rutile increased with increasing reaction time, while that for anatase decreased. The mass fraction and crystallite size of the two polymorphs in these hydrolysates were estimated and presented in Table 2. Clearly, the majority of the hydrolysate obtained in the early stage was anatase. However, with increasing reaction time,

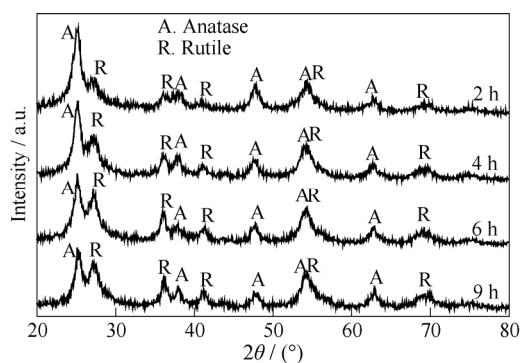


Fig. 6. XRD patterns of hydrolysates at different reaction time durations.

Table 2. Variation of the phase composition and crystallite size of hydrolysates with reaction time

Reaction time / h	Composition / wt%		Crystallite size / nm	
	Anatase	Rutile	Anatase	Rutile
2	78	22	8	6
4	49	51	10	7
6	42	58	8	7
9	35	65	9	6

the rutile phase increased. Upon the reaction time being 9 h, the rutile content rose to 65wt%.

SEM images of hydrolysates obtained at different reaction time durations are shown in Fig. 7. Clearly, the particles gradually grew up and became smooth with increasing reaction time, suggesting that the particle growth might dominate the later hydrolysis, while nucleation is the major hydrolysis process in the early stage.

To understand the variation of polymorph composition with reaction time, an additional experiment was performed. 300 mL of 5wt% H₂SO₄ solution was preheated to 100°C, to which the titanyl sulfate stock solution was added at 2 mL/h.

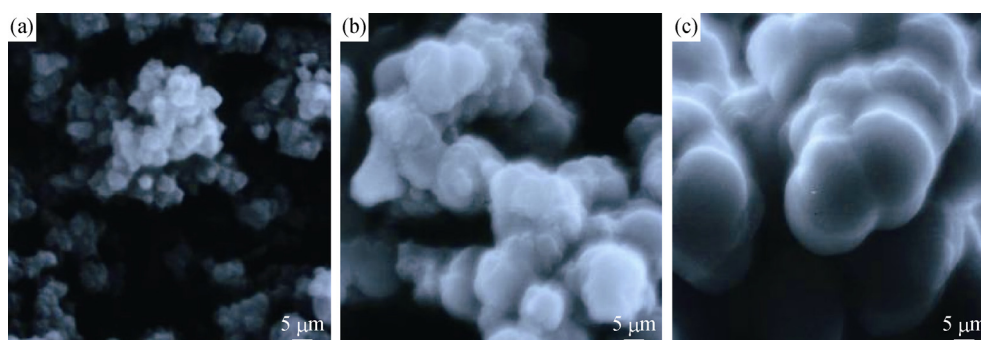


Fig. 7. SEM images of hydrolysates at different reaction time durations: (a) 2 h; (b) 4 h; (c) 9 h.

The feeding terminated in 4 h, and about half of the reacting slurry was withdrawn and separated. The remaining one was unceasingly annealed at 100°C for 5 h and then separated. The two hydrolysate samples thus obtained were characterized using XRD analysis. It was found that they had almost identical phase compositions. The results indicated that anatase precipitated in the initial 4 h did not transform to rutile under the experimental conditions employed. Therefore, the increase of rutile content in the later stage is due to direct formation of more rutile phase on the surfaces of initially precipitated hydrolysate particles.

3.3. Effect of adding rutile crystal seeds

A series of tests was conducted in 5wt% sulfuric acid solution at 100°C with a titanyl sulfate stock solution feeding rate of 2 mL/h for 9 h. Rutile crystal seeds described in Section 2.1 were added before dripping the stock solution. The seed dosages were 0.35wt%, 0.69wt%, 1.04wt%, and 1.38wt%, respectively, of the theoretical amount of the hydrolysate, which could be obtained by complete hydrolysis of 18 mL of the stock solution.

The variation of titanium concentration in the reacting slurry with time was detected and shown in Fig. 8. Unlike hydrolysis in the absence of crystal seeds, the titanium ion concentration increased almost monotonously over the whole reaction time, indicating that hydrolysis occurred in the very early time. Clearly, the introduction of nuclei can overcome the energy barrier of homogeneous nucleation and thus shorten the hydrolysis induction period. With increasing crystal seed dosages, the titanium concentration decreased due to the enhancement of hydrolysis. Based on Fig. 8, the variation of hydrolysis fraction with time was calculated and is shown in Fig. 9. It can be seen that hydrolysis in the presence of seeds occurred at ~0.5 h and conducted almost at a constant rate. Comparatively, hydrolysis in the absence of seeds was delayed for about 1 h and had the highest hydrolysis rate in the initial stage due to high super-

saturation. Besides, it was noticed that the hydrolysis rate slightly increased with increasing seed dosages.

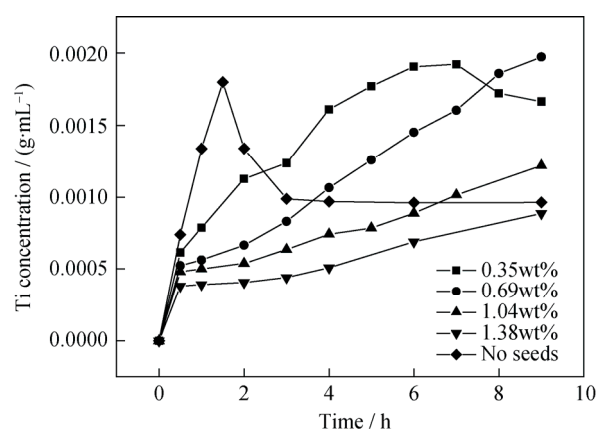


Fig. 8. Variation of the titanium concentration of the reacting slurry with time at different crystal seed dosages.

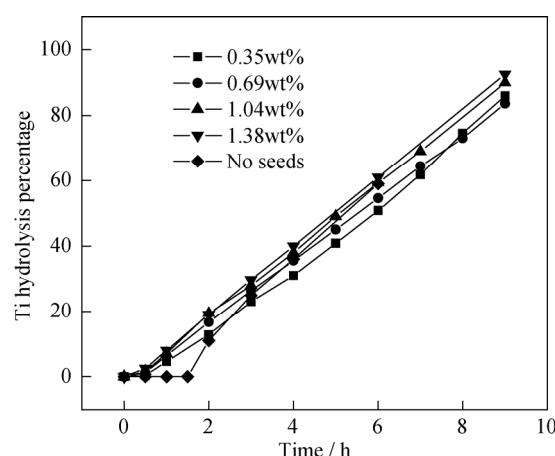


Fig. 9. Variation of the hydrolysis percentage with time at different crystal seed dosages.

XRD patterns of hydrolysates obtained at different seed dosages in 9 h of reaction are shown in Fig. 10. Based on the patterns, the phase percentage and crystallite size of both rutile and anatase in these samples were estimated and are listed in Table 3. Obviously, the addition of rutile crystal

seeds strongly influenced the phase composition. The rutile content decreased with the increasing dosage of crystal seeds under the employed experimental conditions. Upon the dosage of 1.38wt%, the rutile phase content was actually lower than that without the seeds. The reason will be discussed later.

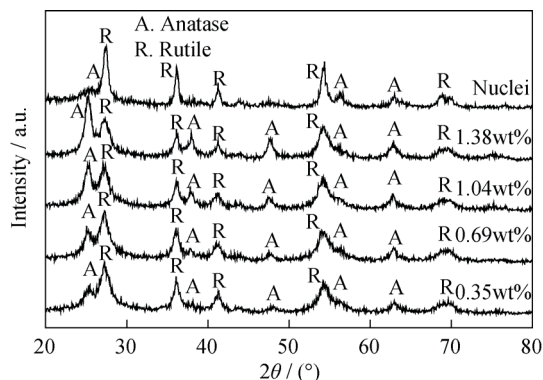


Fig. 10. XRD patterns of hydrolysates at different crystal seed dosages.

Table 3. Variation of the phase composition and crystallite size of hydrolysates with crystal seed dosage

Seed dosage / wt%	Composition / wt%		Crystallite size / nm	
	Anatase	Rutile	Anatase	Rutile
nuclei	0	100	—	16
0	35	65	9	6
0.35	13	87	11	12
0.69	18	82	10	8
1.04	26	74	9	6
1.38	42	58	10	8

3.4. Effect of sulfuric acid concentration

A series of tests was conducted in different sulfuric acid concentration solutions at 100°C with the stock solution feeding rate of 2 mL/h for up to 9 h. The applied acid concentrations were 0wt%, 2.5wt%, 5wt%, 10wt%, and 15wt%, respectively.

XRD patterns of hydrolysates obtained are shown in Fig. 11. Based on the patterns, the phase percentage and crystallite size of both rutile and anatase in these hydrolysates were estimated and are listed in Table 4. The acid concentration significantly affected the phase composition. The maximum rutile content (87%) occurred in the sample obtained in 2.5wt% acid. Increasing or decreasing the acid concentration further would lead to a decrease in rutile content. In both 15wt% sulfuric acid and acid-free solutions, nearly phase-pure anatase could be obtained.

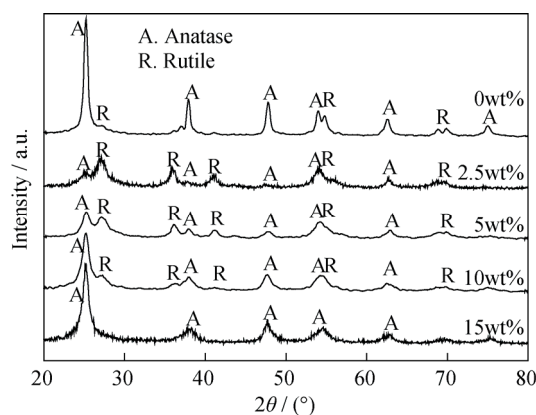


Fig. 11. XRD patterns of hydrolysates at different H₂SO₄ concentrations.

Table 4. Variation of the phase composition and crystallite size of hydrolysates with H₂SO₄ concentration

H ₂ SO ₄ concentration / wt%	Composition / wt%		Crystallite size / nm	
	Anatase	Rutile	Anatase	Rutile
0	96	4	22	—
2.5	13	87	8	7
5	35	65	9	6
10	82	18	11	2
15	99	1	10	—

The variation of titanium ion concentration in the reacting slurry with time at different acid concentrations is shown in Fig. 12. In the acid-free solution, the titanium concentration almost kept close to zero over the whole reacting stage, indicating that the titanyl sulfate hydrolyzed immediately as soon as it was added. With increasing acid concentration, the titanium concentration gradually increased due to increasing titanium stability. A peak value of titanium concentration was observed, which rapidly increased with increasing acid concentration. Clearly, evident titanium

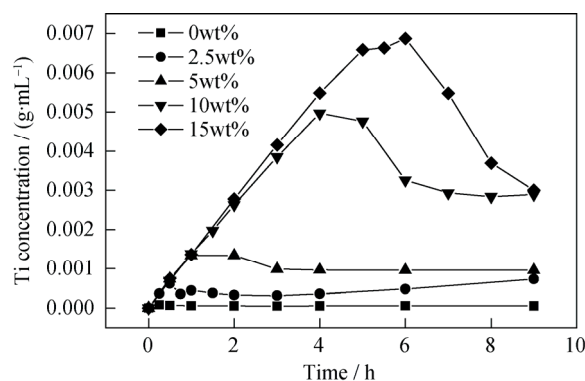


Fig. 12. Variation of the titanium concentration of the reacting slurry with time at different H₂SO₄ concentrations.

hydrolysis started from the peak and speeded up with increasing acid concentration as indicated by the steep slope.

Based on Fig. 12, the variation of hydrolysis fraction with time was calculated and is shown in Fig. 13. It should be noted that since hydrolysis in the acid-free solution was extremely fast, the rate could not be calculated from Fig. 12. Therefore, an additional experiment was conducted, in which 18 mL of the titanium stock solution were rapidly poured into 300 mL acid-free water, which had been preheated to 100°C. The reacting slurry was periodically sampled at the very beginning of the reaction with very short intervals for analyzing the titanium concentration. The result was used to approximately represent hydrolysis with 18 mL stock solution dripping into the acid-free solution at 2 mL/h and is also shown in Fig. 13.

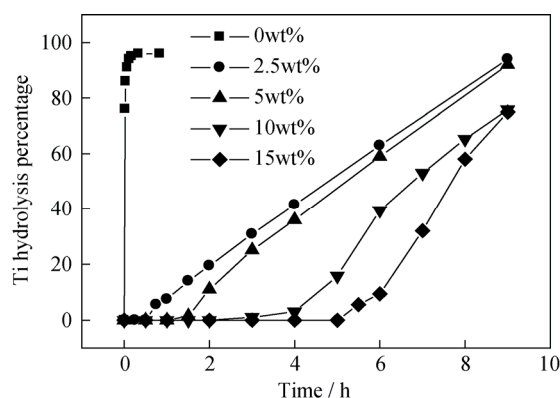


Fig. 13. Variation of the hydrolysis percentage with time at different H_2SO_4 concentrations.

It was noticed that hydrolysis in the solutions of different acid concentrations conducted almost at a constant rate once it started. Hydrolysis in the acid-free solution is the fastest, while the one in the 2.5% acid solution is the slowest. Beyond 2.5%, the hydrolysis speeded up with the increasing acid concentration.

4. Discussion

As is well known, macrocrystalline rutile is a thermodynamically stable phase compared with macrocrystalline anatase or brookite due to its low bulk Gibbs free energy (G_b). For an ultrafine TiO_2 system, the Gibbs free energy (G) comprises the bulk free energy (G_b) and the surface free energy (G_s). Thus, the G_s item is determinant of the phase stability. Since anatase has a lower G_s in air than rutile and brookite, anatase may reverse to be a stable phase when the TiO_2 size is very small. Therefore, the phase stability of polymorph titania is size dependent [6-10]. Zhang and Ban-

field [8] further quantified the size dependence under gaseous atmosphere as follows: anatase, brookite, and rutile are thermodynamically stable, respectively, at grain sizes of <11, between 11 and 35, and >35 nm.

However, in the present study with different titanium stock solution feeding rates, different acid concentrations, and different crystal seed dosages, the crystallite size of hydrous TiO_2 obtained in aqueous solution environment varied only between 2 and 12 nm (see Tables 1-4), and the relationship between TiO_2 polymorphs and crystallite size did not obey the rule established by Zhang and Banfield [8].

Finnegan *et al.* [16] demonstrated that the phase stability of nanosized titania in aqueous solutions was pH dependent. In very acidic solutions, such as pH ~1.0, which is far less than the isoelectric pH value of titania (pH 5.9 for rutile and pH 6.3 for anatase [31]), rutile is more stable than anatase at small size. However, in the present study with a similar acidic environment, lots of anatase hydrolysates were obtained.

Therefore, in the present study, the relationship between TiO_2 phase and hydrolysis conditions cannot be explained only from thermodynamic view.

It was reported that the crystallization rate could affect the crystal phase composition [32-33]. In the present study, the phase state of TiO_2 hydrolysates was influenced by the feeding rate of the titanium stock solution, the dosage of crystal seeds, and the concentration of sulfuric acid. It seems that the hydrolysis rate exerted a very important effect.

To understand the relationship, the average hydrolysis rates under different conditions were calculated from Figs. 2, 9, and 13 and correlated with the rutile phase content in the corresponding hydrolysates as shown in Fig. 14. In all the cases, the rutile phase constitution decreased with increasing hydrolysis rate. In Fig. 14(a), at the Ti feeding rate of 1 mL/h, the average hydrolysis rate of titanium expressed by TiO_2 is about 0.01 g/(L·min), and the rutile content is up to 92%. Upon the feeding rate being 8 mL/h, the average hydrolysis rate increases to 0.075 g/(L·min), and the rutile content drops to the minimum of 2%. In Fig. 14(b), the slowest average hydrolysis rate of 0.02 g/(L·min) is obtained at the 0.35wt% crystal seed dosage with the rutile content of as high as 87%. Upon the seed dosage of 1.38wt%, the average hydrolysis rate increases to 0.028 g/(L·min) with the rutile content dropping to 58%. In Fig. 14(c), the slowest average hydrolysis rate of 0.02 g/(L·min) is obtained at the 2.5wt% acid concentration with as high as 87% of rutile content. Upon the acid concentration of 15wt%, the average hydrolysis rate rises to 0.04 g/(L·min) with the rutile content

reducing to ~1wt%. In the acid-free solution, the fastest average hydrolysis rate of 1.61 g/(L·min) is achieved with the rutile content of as low as 4wt%. Besides, it was noticed that the instantaneous hydrolysis rate (represented by the curve's

slope) actually decreases with prolonging reaction time as shown in the 2 mL/h curve in Fig. 2, and the trend is in good agreement with that of increasing rutile content shown in Table 2.

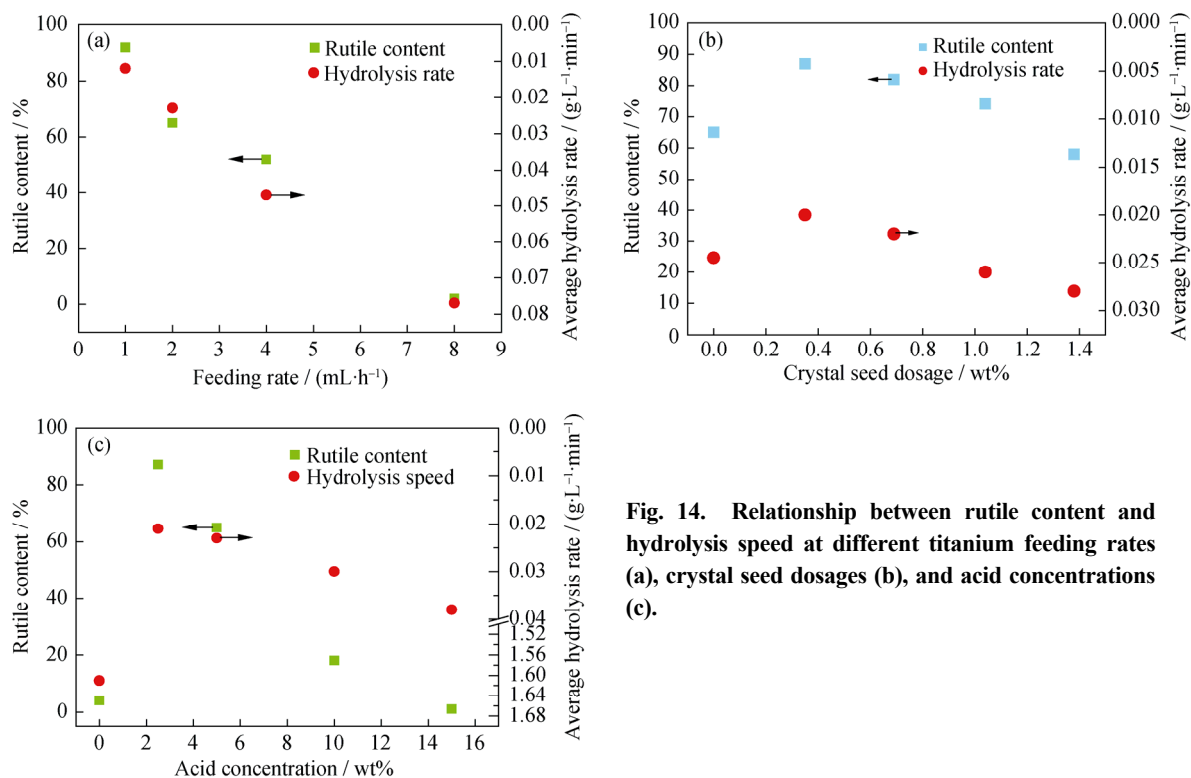


Fig. 14. Relationship between rutile content and hydrolysis speed at different titanium feeding rates (a), crystal seed dosages (b), and acid concentrations (c).

Therefore, a high titanium hydrolysis rate is always favorable for anatase formation. The phase state of hydrolysates obtained at 100°C in 2.5wt% to 15wt% sulfuric acid solutions is almost phase-pure anatase when the hydrolysis rate is more than or equal to 0.04 g/(L·min), while the main phase state is rutile when the hydrolysis rate is ≤0.01 g/(L·min). Upon the hydrolysis rate between 0.02 and 0.03 g/(L·min), the hydrolysate contains almost equal magnitude of rutile and anatase.

In the hydrolysis section of the commercial sulfate process, the titanium-containing solution is generally composed of 230 to 260 g/L TiO₂ and about 10% H₂SO₄ and hydrolyzes at 96°C to 110°C for 4 to 6 h with a hydrolysis percentage of approximate 95% [25]. The hydrolysis rate was calculated to be about 0.77 g/(L·min). According to the criterion established in the present study, we can explain why only the hydrolysate in anatase state is obtained.

The present work demonstrates that although rutile phase is thermodynamically stable in very acidic solutions and can be formed through slow titanium hydrolysis, anatase phase can also be obtained preferentially if the hydrolysis is fast

enough. In other words, anatase is a kinetically stable phase [34-35].

5. Conclusion

Polymorphic hydrous TiO₂ was prepared via thermal hydrolysis of titanyl sulfate and sulfuric acid solutions. The hydrolysis parameters such as the feeding rate of titanyl sulfate, the concentration of sulfuric acid, and seed dosage of rutile crystals significantly influenced the TiO₂ phase state. The reasons behind might be the hydrolysis rate. When the hydrolysis rate is below 0.01 g/(L·min), a hydrolysate with the main crystal phase of rutile is formed. Upon the hydrolysis rate over 0.04 g/(L·min), phase-pure anatase can be obtained. With the hydrolysis rate between 0.02 and 0.03 g/(L·min), the hydrolysate contains almost equal magnitude of rutile and anatase.

References

- [1] M.R. Hoffmann, S.T. Martin, W. Choi, and D.W. Bahnemann, Environmental applications of semiconductor photocatalysis, *Chem. Rev.*, 95(1995), No.1, p.69.
- [2] M. Muneer, S. Das, V.B. Manilal, and A. Haridas,

- Photocatalytic degradation of waste-water pollutants: titanium dioxide-mediated oxidation of methyl vinyl ketone, *J. Photochem. Photobiol. A*, 63(1992), No.1, p.107.
- [3] P. Pichat, J. Disdier, C. Hoang-Van, D. Mas, G. Goutailler, and C. Gaysse, Purification/deodorization of indoor air and gaseous effluents by TiO₂ photocatalysis, *Catal. Today*, 63(2000), No.2-4, p.363.
 - [4] C.J. Barbé, F. Arendse, P. Comte, M. Jirousek, F. Lenzmann, V. Shklover, and M. Grätzel, Nanocrystalline titanium oxide electrodes for photovoltaic applications, *J. Am. Ceram. Soc.*, 80(1997), No.12, p.3157.
 - [5] R.R. Bacsá and M. Grätzel, Rutile formation in hydrothermally crystallized nanosized titania, *J. Am. Ceram. Soc.*, 79(1996), No.8, p.2185.
 - [6] H.Z. Zhang and J.F. Banfield, Polymorphic transformations and particle coarsening in nanocrystalline titania ceramic powders and membranes, *J. Phys. Chem. C*, 111(2007), No.18, p.6621.
 - [7] H.Z. Zhang and J.F. Banfield, Understanding polymorphic phase transformation behavior during growth of nanocrystalline aggregates: Insights from TiO₂, *J. Phys. Chem. B*, 104(2000), No.15, p.3481.
 - [8] H.Z. Zhang and J.F. Banfield, Thermodynamic analysis of phase stability of nanocrystalline titania, *J. Mater. Chem.*, 8(1998), No.9, p.2073.
 - [9] A.K. Vasudevan, P.P. Rao, S.K. Ghosh, G.M. Anilkumar, A.D. Damodaran, and K.G.K. Warriar, Effect of addition of silver on anatase-rutile transformation as studied by impedance spectroscopy, *J. Mater. Sci. Lett.*, 16(1997), No.1, p.8.
 - [10] M.R. Ranade, A. Navrotsky, H.Z. Zhang, J.F. Banfield, S.H. Elder, A. Zaban, P.H. Borse, S.K. Kulkarni, G.S. Doran, and H.J. Whitfield, Energetics of nanocrystalline TiO₂, *Proc. Natl. Acad. Sci. USA*, 99(2002), p.6476.
 - [11] P.K. Naicker, P.T. Cummings, H.Z. Zhang, and J.F. Banfield, Characterization of titanium dioxide nanoparticles using molecular dynamics simulations, *J. Phys. Chem. B*, 109(2005), No.32, p.15243.
 - [12] K.N.P. Kumar, Growth of rutile crystallites during the initial stage of anatase-to-rutile transformation in pure titania and in titania-alumina nanocomposites, *Scripta Metall. Mater.*, 32(1995), No.6, p.873.
 - [13] A.A. Gribb and J.F. Banfield, Particle size effects on transformation kinetics and phase stability in nanocrystalline TiO₂, *Am. Mineral.*, 82(1997), No.7-8, p.717.
 - [14] F. Bregani, C. Casale, L.E. Depero, I. Natali-sora, D. Robba, L. Sangaletti, and G.P. Toledo, Temperature effects on the size of anatase crystallites in Mo-TiO₂ and W-TiO₂ powders, *Sens. Actuators B*, 31(1996), No.1-2, p.25.
 - [15] K. Yanagisawa and J. Ovenstone, Crystallization of anatase from amorphous titania using the hydrothermal technique: effects of starting material and temperature, *J. Phys. Chem. B*, 103(1999), No.37, p.7781.
 - [16] M.P. Finnegan, H.Z. Zhang, and J.F. Banfield, Phase stability and transformation in titania nanoparticles in aqueous solutions dominated by surface energy, *J. Phys. Chem. C*, 111(2007), No.5, p.1962.
 - [17] E. Santacesaria, M. Tonello, G. Storti, R.C. Pace, and S.J. Carra, Kinetics of titaniumdioxideprecipitation by thermalhydrolysis, *J. Colloid Interface Sci.*, 111(1986), No.1, p.44.
 - [18] E. Matijević, M. Budnick, and L. Meites, Preparation and mechanism of formation of titanium dioxide hydrosols of narrow size distribution, *J. Colloid Interface Sci.*, 61(1977), No.2, p.302.
 - [19] L.I. Bekkerman, I.P. Dobrovol'skii, and A.A. Ivakin, Effect of the composition of titanium(IV) solution and conditions of precipitation on the structure of the solid phase, *Russ. J. Inorg. Chem.*, 21(1976), p.223.
 - [20] W. Qin, J.J. Liu, S.L. Zuo, Y.C. Yu, and Z.P. Hao, Solvothermal synthesis of nanosized TiO₂ particles with different crystal structures and their photocatalytic activities, *J. Inorg. Mater.*, 22(2007), No.5, p.931.
 - [21] S.D. Park, Y.H. Cho, W.W. Kim, and Kim S.J., Understanding of homogeneous spontaneous precipitation for monodispersed TiO₂ ultrafine powders with rutile phase around room temperature, *J. Solid State Chem.*, 146(1999), No.1, p.230.
 - [22] A.W. Hixson and J.D. Stetkewicz, Titanium sulfate solutions, *Ind. Eng. Chem.*, 32(1940), No.7, p.1009.
 - [23] A.W. Hixson and W.W. Plechner, Hydrated titanium oxide, thermal precipitation from titanium sulfate solutions, *Ind. Eng. Chem.*, 25(1933), No.3, p.262.
 - [24] A.W. Hixson and R.E.C. Fredrickson, Hydrolysis of titanyl sulfate solutions, *Ind. Eng. Chem.*, 37(1945), No.7, p.678.
 - [25] B. Jells, *Titanium: Its Occurrence, Chemistry and Technology*, Ronald Press, New York, 1966, p.168.
 - [26] J. Amigó, J. Clausell, V. Esteve, J.M. Delgado, M.M. Reventós, L.E. Ochando, T. Debaerdemaeker, and F. Martí, X-ray powder diffraction phase analysis and thermomechanical properties of silica and alumina porcelains, *J. Eur. Ceram. Soc.*, 24(2004), No.1, p.75.
 - [27] R.J. Hill and C.J. Howard, Quantitative phase analysis from neutron powder diffraction data using the Rietveld method, *J. Appl. Cryst.*, 20(1987), No.6, p.467.
 - [28] L.J. Kirwan, F.A. Deeney, G.M. Croke, and K. Hodnett, Characterisation of various Jamaican bauxite ores by quantitative Rietveld X-ray powder diffraction and ⁵⁷Fe Mossbauer spectroscopy, *Int. J. Miner. Process.*, 91(2009), No.1-2, p.14.
 - [29] L. Lutterotti and P. Scardi, Simultaneous structure and size-strain refinement by the Rietveld method, *J. Appl. Cryst.*, 23(1990), No.4, p.246.
 - [30] H. Rietveld, Line profiles of neutron powder-diffraction peaks for structure refinement, *Acta Cryst.*, 22(1967), No.1, p.151.
 - [31] K. Bourikas, T. Hiemstra, and W.H. Van Riemsdijk, Ion pair formation and primary charging behavior of titanium oxide (anatase and rutile), *Langmuir*, 17(2001), No.3, p.749.
 - [32] B. Katerska, G. Exner, E. Perez, and M.N. Krasteva, Cooling rate effect on the phase transitions in a polymer liquid crystal: DSC and real-time MAXS and WAXD experiments, *Eur. Polym. J.*, 46(2010), No.7, p.1623.
 - [33] V. Andronis and G. Zografí, Crystal nucleation and growth of indomethacin polymorphs from the amorphous state, *J. Non Cryst. Solids*, 271(2000), No.3, p.236.
 - [34] K. Yanagisawa and J. Ovenstone, Crystallization of anatase from amorphous titania using the hydrothermal technique: Effects of starting material and temperature, *J. Phys. Chem. B*, 103(1999), No.37, p.7781.
 - [35] C. Wang, Z.X. Deng, G.H. Zhang, S.S. Fan, and Y.D. Li, Synthesis of nanocrystalline TiO₂ in alcohols, *Powder Technol.*, 125(2002), No.1, p.39.